Archives of Biochemistry and Biophysics 529 (2013) 112–121

Contents lists available at SciVerse ScienceDirect

Archives of Biochemistry and Biophysics

journal homepage: www.elsevier.com/locate/yabbi

Stereochemical mechanism of two sabinene hydrate synthases forming antipodal monoterpenes in thyme (*Thymus vulgaris*)

Sandra T. Krause [a], Tobias G. Köllner [a,1], Julia Asbach [b], Jörg Degenhardt [a,*]

[a] Martin Luther University Halle-Wittenberg, Institute for Pharmacy, Hoher Weg 8, D-06120 Halle/Saale, Germany
[b] Max Planck Institute for Chemical Ecology, Hans-Knöll-Str. 8, D-07745 Jena, Germany

ARTICLE INFO

Article history:
Received 12 September 2012
and in revised form 2 December 2012
Available online 12 December 2012

Keywords:
Thymus vulgaris
Monoterpene synthase
Sabinene hydrate
Stereochemical mechanism
Site-directed mutagenesis
Active-site modeling

ABSTRACT

The essential oil of *Thymus vulgaris* consists of a complex blend of mono- and sesquiterpenes that provides the plant with its characteristic aromatic odor. Several chemotypes have been described for thyme. In this study, we identified two enzymes of the sabinene hydrate chemotype which are responsible for the biosynthesis of its major monoterpene alcohols, (1*S*,2*R*,4*S*)-(*Z*)-sabinene hydrate and (1*S*,2*S*,4*R*)-(*E*)-sabinene hydrate. Both TPS6 and TPS7 are multiproduct enzymes that formed 16 monoterpenes and thus cover almost the whole monoterpene spectrum of the chemotype. Although the product spectra of both enzymes are similar, they form opposing enantiomers of their chiral products. Incubation of the enzymes with the potential reaction intermediates revealed that the stereospecificity of TPS6 and TPS7 is determined by the formation of the first intermediate, linalyl diphosphate. Since TPS6 and TPS7 shared an amino acid sequence identity of 85%, a mutagenesis study was employed to identify the amino acids that determine the stereoselectivity. One amino acid position had a major influence on the stereochemistry of the formed products. Based on comparative models of TPS6 and TPS7 protein structures with the GPP substrate docked in the active site pocket, the influence of this amino acid residue on the reaction mechanism is discussed.

Introduction

The essential oil of thyme (*Thymus vulgaris* L.) is a natural resource for a wide range of monoterpenes. Due to their antibacterial and spasmolytic activities, these monoterpenes are used in many pharmaceuticals. In addition, thyme is widely used as a spice and as a preservative in the food industry [1]. The composition of the essential oils varies strongly between thyme plants. Natural populations of thyme often consist of several chemotypes which are morphologically identical sub-populations with a distinct composition of their essential oils. These chemotypes are characterized by their major monoterpene alcohols. In Southern France, six chemotypes of *T. vulgaris* are distinguished: α-terpineol (A-type), carvacrol (C-type), geraniol (G-type), linalool (L-type), thymol (T-type) and sabinene hydrate (U-type) [2].

The structural diversity of monoterpenes is formed by the enzyme class of monoterpene synthases which convert geranyl diphosphate (GPP)[2] to the basic monoterpene olefins or alcohols [3]. The terpene synthase reaction mechanism that realizes this diversity of structures has been in the focus of intensive research in the last years [4]. The reactions start with the ionization of the 2,3-(*E*)-GPP substrate in the presence of a divalent cation. The resulting carbocationic intermediate is highly reactive and undergoes a series of cyclizations, hydride shifts, and rearrangements to form the basic carbon skeletons of the monoterpenes. The reactions are terminated by deprotonation, additional endocylizations, or water capture which leads to the formation of monoterpene alcohols [3]. A feature unique to terpene synthases is the formation of multiple products. One terpene synthase can generate complex terpene blends with over 50 compounds [5]. Most terpene synthases have a stereoselective reaction mechanism. The resulting monoterpene enantiomers can differ from each other in their function in plant insect-interactions [6] and are sometimes distinguished by their smell [7].

Many monoterpene synthases convert the achiral GPP substrate to compounds that contain one or more stereocenters. Studies on a fenchol synthase from fennel [8], bornyl diphosphate synthases

* Corresponding author. Fax: +49 345 5527407.
E-mail address: joerg.degenhardt@pharmazie.uni-halle.de (J. Degenhardt).
[1] Present address: Max Planck Institute for Chemical Ecology, Hans-Knöll-Str. 8, D-07745 Jena, Germany.

[2] *Abbreviations used:* GPP, geranyl diphosphate; LPP, linalyl diphosphate; TPS, terpene synthase; RACE, rapid amplification of cDNA ends; GC–MS, gas chromatography–mass spectrometry; SPME, solid phase micro extraction; DTT, dithiothreitol; PMSF, phenylmethylsulfonylfluorid.

0003-9861/$ - see front matter © 2012 Elsevier Inc. All rights reserved.
http://dx.doi.org/10.1016/j.abb.2012.12.003

from tansy and sage [9], or α-pinene synthases of loblolly pine [6] suggested that the stereospecificity of the enzyme reaction is defined in the early steps of the pathway, by the initial folding of GPP in the active-site pocket. The right-handed folding of GPP in the active site leads to the formation of (3*S*)-linalyl diphosphate ((3*S*)-LPP) and the left handed folding leads to (3*R*)-linalyl diphosphate ((3*R*)-LPP), the first chiral intermediates in the pathway (Fig. 1).

Although a large number of plant terpene synthases has been identified to date, little is known about the structure–function relationships in the active center of these enzymes and their impact on product specificity and stereoselectivity [4]. Some conserved sequence motifs and their catalytic function have been identified, like the the magnesium-binding DDxxD and NSE/DTE motifs which are highly conserved among terpene synthases [4,10]. Together, these motifs bind three magnesium ions which interact with the diphosphate moiety of the substrate and cause the initial ionization and rearrangement of the diphosphate group [11]. Another motif typical for monoterpene synthases is the RRx_8W-motif which is located 60 amino acids from the N-terminus. This motif is important for the isomerization of the GPP substrate to the linalyl cation intermediate [12,13]. In monoterpene synthases, site-directed mutagenesis and domain swapping have been utilized to identify structural elements that determine product specificity [14–18]. However, none of these studies reported on structural elements of monoterpene synthases which influence the stereochemical configuration of terpenes.

Here, we describe the isolation and biochemical characterization of two sabinene hydrate synthases from the sabinene hydrate chemotype of *T. vulgaris*. The opposite stereoselectivity of the enzymes provided a chance to investigate the structural base for their stereospecificity. We demonstrated that the stereospecificity is determined by the initial conformation of the GPP substrate in the active site. Mutagenesis experiments revealed a single amino acid residue that determined the stereochemical configuration of terpene products.

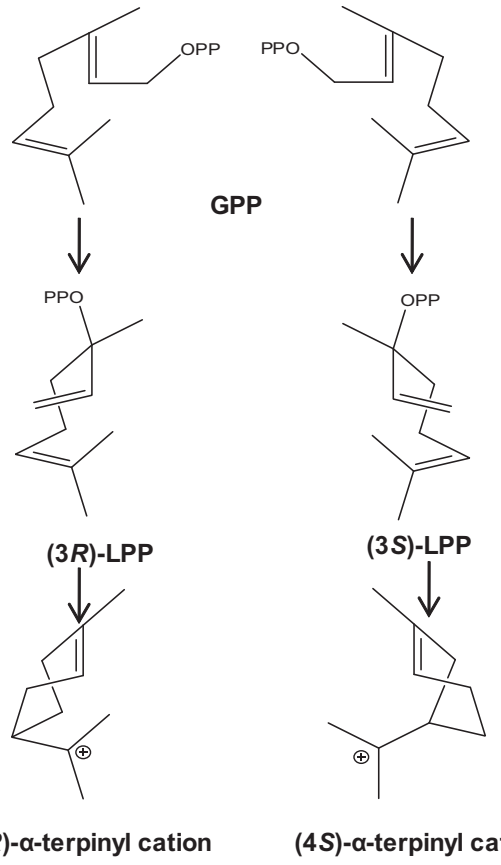

Fig. 1. The binding conformation of GPP determines the stereochemical conformation of LPP which is converted to the respective enantiomers of the α-terpinyl cation intermediate.

Materials and methods

Plant material

The chemotypes of thyme (*T. vulgaris*) were collected and characterized for their terpene content in Southern France at CNRS, Montpellier, France [19]. Plants were grown in the greenhouse under following conditions: temperature day (13 h light) 20–22 °C, temperature night 18–20 °C, humidity 55%, luminosity approximately 320 μmol photosynthetically active radiation.

Sequence isolation and phylogenetic analysis

For the isolation of terpene synthase genes, 5′and 3′-RACE-libraries of the sabinene hydrate chemotype were generated. The libraries were constructed with the SMARTer RACE cDNA Amplification Kit (Clontech, Mountain View, CA, USA). For the first PCR, degenerate primers based on sequences of terpene synthase genes from other Lamiaceae (Table S1) were used to obtain partial 3′-sequences. The components of the PCR reaction were: 0.8 μl Advantage Taq DNA Polymerase Mix (5 U/μl), 4 μl Advantage Taq PCR buffer, 1 μl dNTPs (10 mM each), 1 μl universal primer mix and 1 μl gene-specific fwd-primer (10 pmol/μl) (Table S1), 3 μl 3′-RACE cDNA and PCR grade water added to a final volume of 40 μl. The PCR was conducted with an initial denaturation at 95 °C for 2 min, 30–35 cycles of denaturation at 95 °C for 30 s, annealing ranging from 48 to 60 °C for 30 s, extension at 68 °C for 2 min, and a final step at 68 °C for 5 min. The PCR fragments were cloned into the pCR4-TOPO vector (TOPO TA cloning kit for sequencing, Invitrogen, Carlsbad, CA, USA) and subsequently sequenced. The obtained sequences were compared by BLAST searches via the NCBI sequence database [20] and showed similarity to monoterpene synthases from other plants. The sequence fragments were used to design primers for the isolation of the 5′ends of the full length gene. This time, the components of the PCR reaction were: 1 μl Advantage Taq DNA Polymerase Mix (5 U/μl), 5 μl Advantage Taq PCR buffer, 1 μl dNTPs (10 mM each), 5 μl universal primer mix and 1 μl gene-specific primer (10 pmol/μl) (Table S1), 2.5 μl 5′-RACE cDNA and PCR grade water added to a final volume of 50 μl. PCR thermocycles were run as follows: initial denaturation at 95 °C for 2 min, 30–35 cycles of denaturation at 94 °C for 30 s, annealing ranging from 64 to 68 °C for 30 s, extension at 72 °C for 1.5 min, and a final step at 72 °C for 5 min. PCR fragments were cloned into pCR4-TOPO vector and sequenced. All 5′end and 3′end sequences were assembled with the SeqMan program (Lasergene DNAStar V5.05, Madison, WI, USA). This assembly revealed two open-reading frames called *tps*6 and *tps*7.

Amino acid sequence alignments and the neighbor-joining tree were constructed using MegAlign software (Lasergene DNAStar V5.05, Madison, WI, USA) and the ClustalW method (protein weight matrix: Gonnet series, gap penalty: 10.00, gap length penalty: 0.20, delay divergent sequences: 30%).

RNA extraction from leaf material and cDNA synthesis

Total RNA was extracted from 100 mg homogenized *T. vulgaris* young leaves pooled from five plants. The RNA was extracted with the RNeasy Plant Mini Kit (Qiagen, Hilden, Germany). To remove residual genomic DNA, RNA was treated with RQ1 RNAse-free

DNAse (Promega GmbH, Mannheim, Germany). RNA was quantified by spectrophotometry using the NanoQuant infinite M200 (Tecan, Männedorf, Switzerland). For cDNA synthesis, the Fermentas First Strand cDNA Kit (Fermentas, St. Leon-Rot, Germany) was used according to the manufacturer's instructions.

Transcript quantification by qRT-PCR

Transcript quantification was performed with a CFX96 Real Time System (BioRAD, München, Germany). The components of the PCR reaction were: 10 µl Maxima SYBR Green/ROX qPCR Master Mix (Fermentas, St. Leon-Rot, Germany), 0.5 µl Primer 1 and 0.5 µl Primer 2 (Table S1), 5 µl template (1:5 diluted) and 4 µl PCR-grade water. Controls included non-template controls (water-template). PCR thermocycles were run as follows: 10 min at 95 °C, 40 cycles of 30 s at 95 °C, 30 s at 62 °C and 40 s at 72 °C. Fluorescence was determined after each extension phase. After each run a melting curve analysis from 60 °C to 95 °C was performed. The amplification products were cloned and sequenced to validate the primer specificity. The amplification plots were analyzed with the BioRAD CFX manager to receive Ct values. For relative qRT-PCR 18S ribosomal RNA was employed as housekeeping gene. Relative quantification of *tps*6 and *tps*7 copy number in each cDNA sample was conducted using a standard curve. The standard curve was generated with cDNA containing the respective genes, therefore a dilution series from 3 to 1/27-fold was made.

Protein overexpression, enzyme purification and enzyme assay

The open reading frames of the putative terpene synthases TPS6 and TPS7 with 5′ signal peptide-truncations (43 amino acids from the N-terminus) were cloned into the bacterial expression vector pASK-IBA37plus (IBAGmbH, Göttingen, Germany). This vector contains a 6xHis-tag and a *tet*-promotor. The genes were amplified with primers created with the "Primer D'Signer" software (IBA GmbH, Göttingen, Germany) (Table S1) using the Go Taq DNA Polymerase (Promega GmbH, Mannheim, Germany). The amplification products were digested and cloned into the pASK-IBA37plus expression vector according to the manufacturer's instructions. The expression constructs were verified by sequencing and transformed into the *Escherichia coli* TOP10 strain (Invitrogen, Carlsbad, CA, USA). A starter culture of 5 ml Luria–Bertani (LB) medium with 100 µg ml^{-1} ampicillin was grown overnight at 37 °C. 3 ml of the starter culture were used to inoculate 100 ml of LB-medium with 100 µg ml^{-1} ampicillin and bacteria were grown at 37 °C to an OD of 0.6. Terpene synthase expression was induced by addition of anhydrotetracycline (final concentration 200 µg/l). The cultures were shaken for 20 h at 18 °C. The cells were harvested by centrifugation for 10 min at 5.000 g and 4 °C. The pellets were resuspended in 3 ml extraction buffer (50 mM Tris–HCl pH 7.5, 10% glycerol, 5 mM $MgCl_2$, 5 mM DTT, 5 mM sodium ascorbate pH 7.0, 0.5 mM PMSF). After disruption by sonification (three times 30 s at 50% power, Branson Sonifier 250, Dietzenbach, Germany), cell fragments were removed by centrifugation at 14,000 rpm and 4 °C for 20 min. The cell extract was transferred into assay buffer (10 mM Tris–HCl pH 7.5, 10% glycerol, 1 mM DTT) with 10DG columns (Bio-Rad Laboratories, Hercules, CA, USA).

For enzyme purification, 4 ml crude enzyme extract was mixed with 5 ml of Profinity IMAC Ni-charged resin (Bio-Rad Laboratories, Hercules, CA, USA). After incubation for 1 h at 4 °C and with shaking at 170 rpm, the resin was transferred to a Poly-Prep Chromatography column (Bio-Rad Laboratories, Hercules, CA, USA) and the enzyme was eluted with elution buffer (50 mM Tris–HCl pH 8.0, 150 mM NaCl, 250 mM imidazol, pH 8.0, 10% glycerol). The enzyme concentration was determined according to a method described by Gill and von Hippel [21].

Enzyme activity assays were performed with 100 µl volume containing 30 µl enzyme crude extract and 70 µl reaction-mix (10 mM Tris–HCl pH 7.5, 10% glycerol, 1 mM DTT, 60 µM GPP (Echelon Research Laboratories, Salt Lake City, USA), 10 mM $MgCl_2$). Enzyme products were collected by a polydimethylsiloxane-coated SPME fiber (SUPELCO, Belafonte, PA, USA). The fiber was exposed in the headspace of the assay mixture for 45 min at 35 °C in a water bath. For quantitative FID-analyses, 400 µl of crude enzyme extract and 600 µl reaction mix (10 mM Tris–HCl pH 7.5, 10% glycerol, 1 mM DTT, 60 µM GPP (Echelon Research Laboratories, Salt Lake City, USA), 10 mM $MgCl_2$) were mixed and overlayed with 300 µl hexane, supplied with 10 µg/ml nonyl acetate as internal standard. The assay was then incubated at 37 °C for 3 h or 20 min for kinetic analyses, respectively. Terpene products were transferred into the organic solvent by shaking intensively for 2 min. 50 µl of hexane were used for GC–FID analysis of contained terpenes.

GC–MS analysis of leaf terpenes and products of terpene synthase assay

Young leaves from three plants of the sabinene hydrate chemotype of *T. vulgaris* were combined and ground to a fine powder with mortar and pestle. The powder (50–100 mg) was soaked in 600 µl hexane and incubated for 1 h at RT. 50 µl of the hexane were used for qualitative GC–MS or quantitative GC–FID analysis of terpenes. Alternatively, a SPME fiber consisting of 100 µm polydimethylsiloxane (SUPELCO, Belafonte, PA, USA) was exposed to the leaf volatiles for 5 s. The terpenes were identified with a gas chromatograph (GC-2010, Shimadzu, Duisburg) coupled to a mass spectrometer (GCMS-QP 2010 Plus, Shimadzu). 1 µl of hexane extract was injected with an injector temperature of 220 °C. Alternatively, a SPME fiber was introduced into the injector. All volatiles were separated on an EC5-MS column (30 m length, 0.25 mm inner diameter and 0.25 µm film) (Grace, Deerfield, IL, USA) and identified with the Shimadzu software "GCMS Postrun Analysis" with the mass spectra libraries "Wiley8" (Hewlett&Packard) and "Adams" [22]. GC-program: 50 °C for 2 min, first ramp 7 °C/min to 150 °C, second ramp 100 °C/min to 300 °C, final 2 min hold. GC–MS carrier gas: hydrogen (1 ml/min). For the analysis of chiral compounds, the Rt-bDex sm column (Restek, Bad Homburg, Germany) was used with the following conditions: GC-program: 50 °C for 1 min, first ramp 2 °C/min to 170 °C, second ramp 100 °C/min to 220 °C, final 2 min hold. GC–MS carrier gas: hydrogen (1 ml/min). Alternative GC-program optimized for chiral separations: 40 °C for 1 min, first ramp 1 °C/min to 120 °C, second ramp 100 °C/min to 220 °C, final 2 min hold, column flow: 2 ml/min. For FID-analyses, the following temperature program was used: 40 °C for 3 min, first ramp 6 °C/min to 280 °C, second ramp 100 °C/min to 300 °C, final 2 min hold.

Stereospecific synthesis of LPP for terpene synthase assays

(3*S*)- and (3*R*)-LPP were synthesized according to a method described by Keller and Thompson [23].

(3*R*)-linalool was purchased from Sigma–Aldrich Co. (St. Louis, MO, USA). Due to the lack of commercially available (3*S*)-linalool, coriander oil (SAFC Supply solutions, St. Louis, MO, USA) was used for phosphorylation. This oil consists mostly of linalool, with an 1:10 enantiomeric ratio of (3*R*/3*S*)-linalool.

Determination of K_m-values

Enzyme (30 µl) crude extract was incubated with 5 mM magnesium and 5 µM GPP between 5 and 30 min to determine the linear phase of the reactions. For the determination of the substrate K_m-values, the enzymes were incubated with 5 mM magnesium and

^{3}H-GPP in a range of 1–30 μM. All assays were overlaid with 1 ml pentane and incubated at 30 °C for 7.5 or 10 min depending on the linear phase for TPS6 and TPS7, respectively. The assays were stopped by shaking at 1.400 rpm for 2 min to partition terpene volatiles in the solvent phase. 500 μl pentane were mixed with 2 ml of scintillation cocktail (RotiSzint2200, Roth, Karlsruhe, Germany) and counts-per-minute were measured in a scintillator (LS 6500, Beckman Coulter Inc., Krefeld). All assays were performed in triplicate. The K_m values were determined by using the Lineweaver–Burke method.

In-vitro-mutagenesis of terpene synthase open reading frames

For site-directed mutagenesis, the Stratagene QuickChange method (Stratagene, La Jolla, USA) was used. The PCR-based mutagenesis protocol was performed with *tps*6 or *tps*7 cDNA cloned into the expression vector pASKIBA37plus. Primers containing the desired mutations are listed in Table S1. The constructs were sequenced before expression to ensure successful mutagenesis.

Modeling of the substrate-binding active site

Models of the three-dimensional structure of TPS6 and TPS7 were generated using the Swiss-Model Server [24–26]. For modeling, the TPS6 and TPS7 amino acid sequences were fitted to the template structure of bornyl diphosphate synthase (PDB code: 1n1zA) [27]. Hydrogen atoms were added to the structures using the program AutoDock Tools [28]. Energy-minimized ligand structures were generated with the software ChemDraw and Chem3D (CambridgeSoft, Cambridge, USA). Docking of the ligands into the model of the TPS6 and TPS7 active site cavity was performed with the program AutoDock Vina [29]. The resulting models were visualized with the program PyMOL [30].

Results

The multiproduct terpene synthases TPS6 and TPS7 provide most of the monoterpene spectrum of the T. vulgaris sabinene hydrate chemotype

To identify the terpene synthase genes of *T. vulgaris* that are responsible for the production of the monoterpenes in the sabinene hydrate chemotype, we generated 5′- and 3′-RACE cDNA libraries from this plant. We conducted 3′-RACE PCRs with degenerated forward-primers based on previously identified terpene synthase genes of Lamiaceae. This screen revealed two fragments of about 1000 bp length, which were extended by 5′-RACE PCRs to the complete open reading frame. The open reading frames of the putative terpene synthases shared a sequence identity of 89% on DNA-level (Fig. S1) and were designated *tps*6 and *tps*7. Towards the C-terminal end of the protein, both sequences contained the magnesium-binding DDxxD-motif typical for terpene synthases. In both sequences, the RRx$_8$W-motif was found 60 amino acids from the N-terminus. According to the prediction by the ChloroP 1.1 database [31], both sequences contained an N-terminal signal peptide of 47 amino acids. Since plastids are the location of monoterpene biosynthesis, we assumed that both *tps*6 and *tps*7 encode monoterpene synthases. This assumption was supported by their high amino acid similarity to monoterpene synthases from other plants, especially from the Lamiaceae family (Fig. 2).

TPS6 and TPS7 were heterologously expressed in *E. coli* after truncation of the first 43 amino acids that may encode the signal peptide. With GPP substrate, both enzymes produced 16 different monoterpenes. The product spectra of TPS6 and TPS7 differed in their major product, sabinene hydrate. TPS6 converted GPP into both (*E*)- and (*Z*)-sabinene hydrate, while TPS7 formed mostly

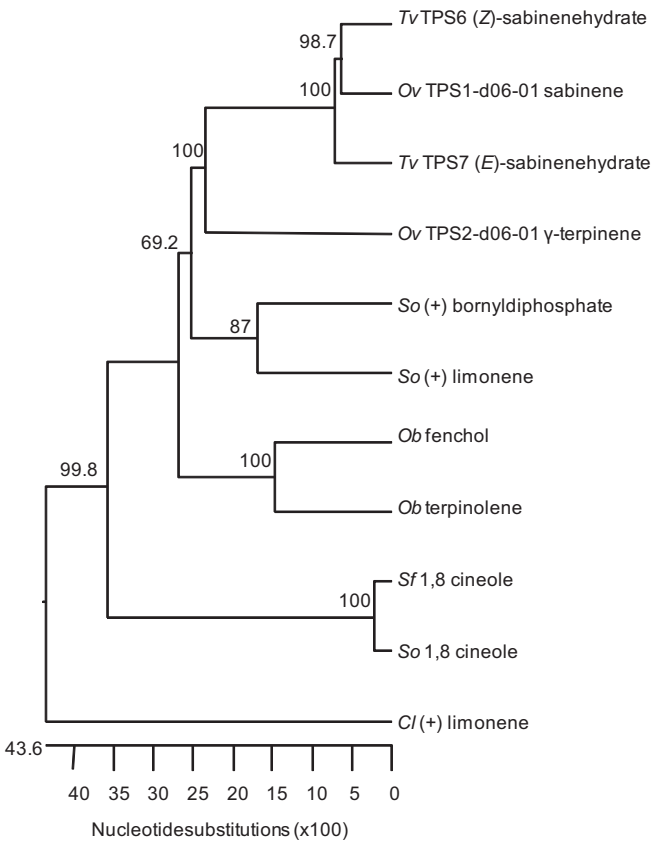

Fig. 2. Neighbor-joining dendrogram with TPS6, TPS7 and monoterpene synthases from other plant species. Each branch is designated with the abbreviation of the species and the main product of the enzyme. Bootstrap values are given as a percentage of 1000 replicates. GenBank IDs: *Cl Citrus limon*: (+)-limonene synthase (GenBank ID: AAM53944); *Ob Ocimum basilicum*: fenchol synthase (GenBank ID: AAV63790), terpinolene synthase (GenBank ID: AAV63792); *Ov Origanum vulgare:* TPS1-d06-01 (GenBank ID: ADK73623), TPS2-d06-01 (GenBank ID: ADK73621); *So Salvia officinalis*: 1,8-cineole synthase (GenBank ID: AAC26016), (+)-bornyl diphosphate synthase (GenBank ID: AAC26017), (+)-sabinene synthase (GenBank ID: AAC26018); *Sf Salvia fruticosa*: 1,8-cineole synthase (GenBank ID: ABH07677); *Tv Thymus vulgaris*: TPS6 (*Z*)-sabinene hydrate synthase (GenBank ID: JX946357), TPS7 (*E*)-sabinene hydrate syntase (GenBank ID: JX946358).

the (*E*)-isomer and only a very small quantity of the (*Z*)-isomer (Fig. 3, Table 1). The most abundant minor products were α-pinene, myrcene, limonene and α-terpineol (Table 1). The product spectra of both enzymes were almost identical with the monoterpene blend of thyme plants of the sabinene hydrate chemotype (Fig. 3, Table 1). Only the *para*-cymene present in the essential oil of the chemotype was not formed by these enzymes. Gene expression analysis by real-time quantitative PCR revealed that both *tps*6 and *tps*7 were expressed at similar levels in leaves of the sabinene hydrate chemotype (Fig. 4). The K_m values of the enzymes, however, displayed significant differences. For TPS6, the K_m value for GPP was 33.5 μM, which is high in comparison to those of other monoterpene synthases. In contrast, the K_m value of TPS7 was determined as 6.1 μM, which is typical for monoterpene synthases [32].

TPS6 and TPS7 produce monoterpenes with opposite stereochemistry

(*E*)- and (*Z*)-sabinene hydrate, the main products of TPS6 and TPS7, have chiral centers at C-1, C-2 and C-4. To compare the enantiomeric compositions of the sabinene hydrate found in the essential oil of the sabinene hydrate chemotype with the ones formed by TPS6 and TPS7, we analyzed the plant's essential oil and TPS6/TPS7

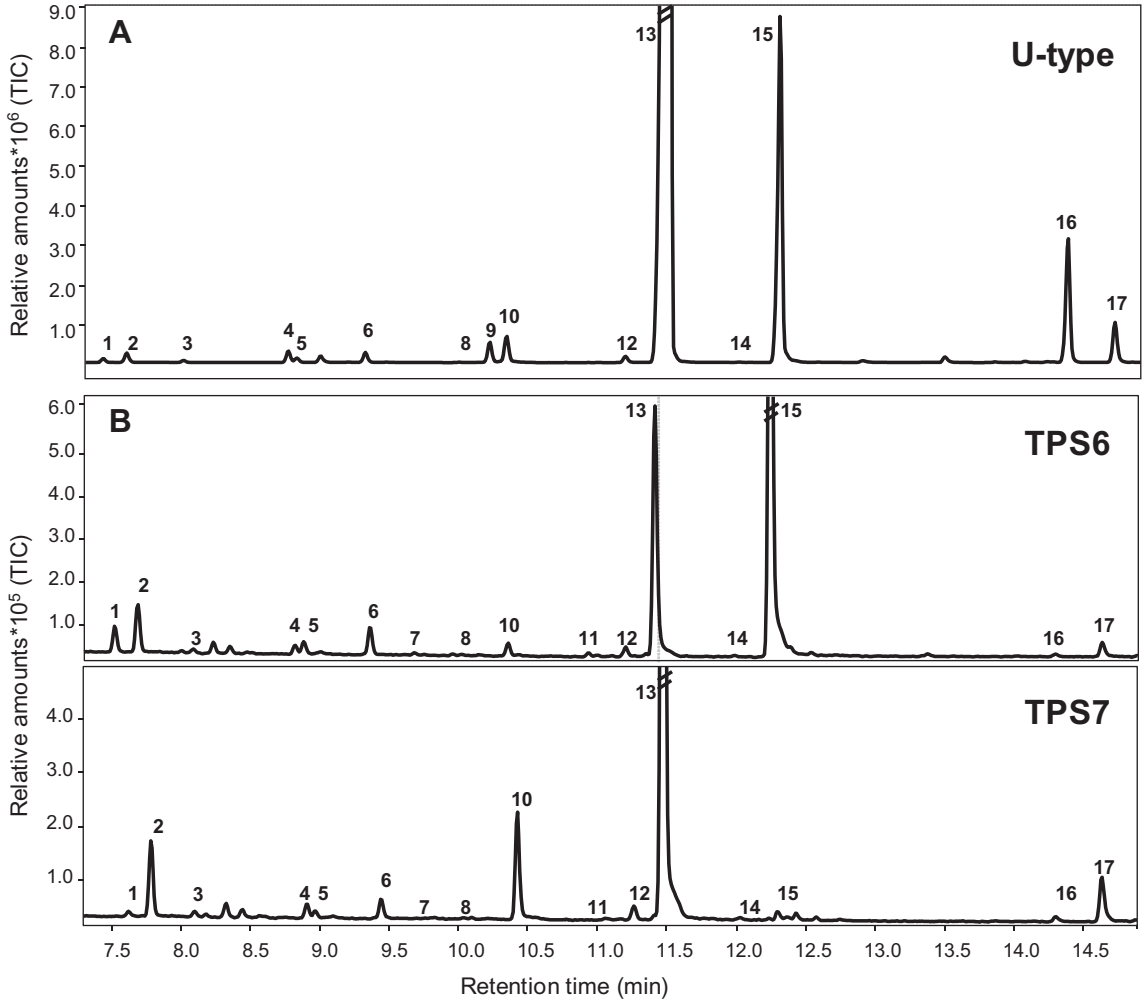

Fig. 3. Monoterpene spectrum of the (*E*)-sabinene hydrate chemotype of *T. vulgaris*. Terpenes were extracted with hexane and analyzed by GC–MS. (A) The terpene synthases TPS6 and TPS7 produce monoterpenes of the (*E*)-sabinene hydrate chemotype of *T. vulgaris*. (B) TPS6 and TPS7 were expressed in *E. coli*, extracted, and incubated with the substrate GPP. The resulting monoterpene products were identified by GC–MS. The numbers given to the peaks refer to the compounds listed in Table 1.

Table 1
Monoterpene composition of the product blends formed by TPS6, TPS7, and the essential oil of the (*E*)-sabinene hydrate chemotype of *T. vulgaris*. The amounts of monoterpenes were determined by GC–FID analysis and are given as a percentage of the total monoterpene content. Nonylacetate (10 μg/ml) was used as an internal standard. N.e.i. = not elsewhere identified.

		U-type [%]	TPS6 [%]	TPS7 [%]
1	α-Thujene	0,64	1,83	0,56
2	α-Pinene	0,95	3,23	3,64
3	Camphene	0,23	0,32	0,23
4	Sabinene	1,50	1,09	0,99
5	β-Pinene	0,48	1,32	0,58
6	Myrcene	1,41	2,60	1,21
7	α-Phellandrene	–	0,43	0,34
8	α-Terpinene	0,65	0,82	0,68
9	*para*-Cymene	2,00	–	–
10	Limonene	3,31	1,97	6,28
11	β-Ocimene	–	0,34	n.e.i.
12	γ-Terpinene	1,65	1,82	1,37
13	(*E*)-Sabinene hydrate	58,01	20,91	77,82
14	Terpinolene	0,33	0,46	0,38
15	(*Z*)-Sabinene hydrate	17,21	60,37	1,43
16	Terpinene-4-ol	8,03	0,82	0,63
17	α-Terpineol	3,58	1,68	3,84

products on a chiral-phase column. Plants of the sabinene hydrate chemotype produced all four stereoisomers of (*E*)- and (*Z*)-sabinene hydrate, with (1*S*,2*S*,4*R*)-(*E*)-sabinene hydrate dominating the

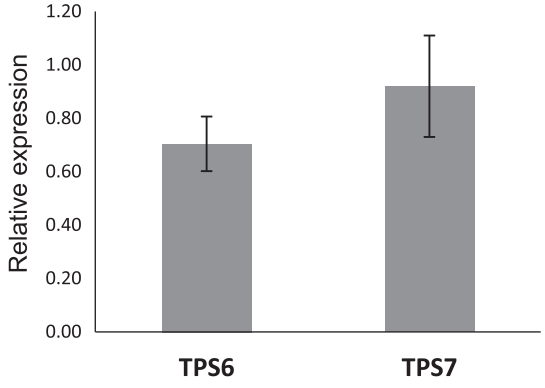

Fig. 4. The monoterpene synthases *tps*6 and *tps*7 are both expressed in leaves of thyme. Transcript concentrations were determined relative to control genes by real-time quantitative PCR.

essential oil (Fig. 5A). After heterologous expression, the terpene synthase TPS6 formed (1*S*,2*R*,4*S*)-(*Z*)-sabinene hydrate as the major product and minor concentrations of both enantiomers of (*E*)-sabinene hydrate. Conversely, TPS7 only produced (1*S*,2*S*,4*R*)-(*E*)-sabinene hydrate, along with traces of (1*S*,2*R*,4*S*)-(*Z*)-sabinene hydrate. The (1*R*,2*S*,4*R*)-isomer of (*Z*)-sabinene hydrate was not de-

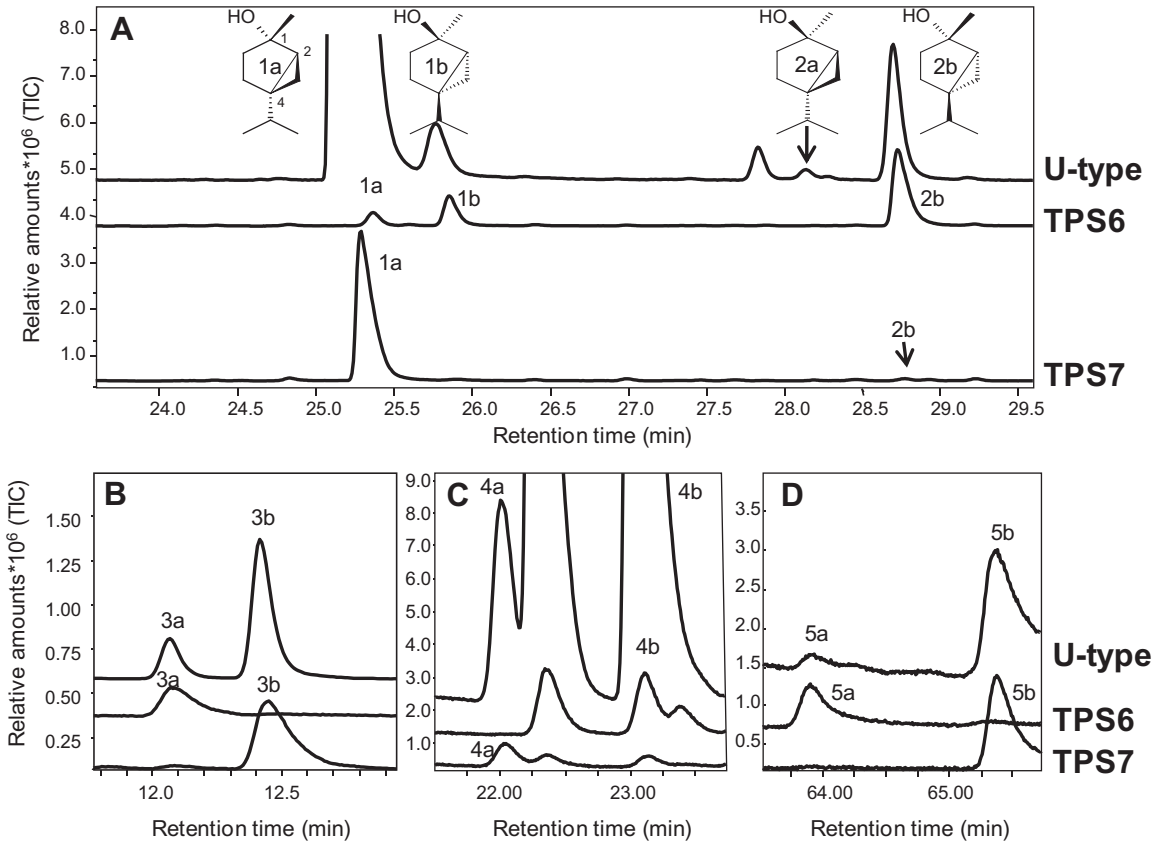

Fig. 5. The enantiomeric composition of sabinene hydrate (A), α-pinene (B), β-pinene (C) and α-terpineole (D) of TPS6 and TPS7 products from GPP, and the (*E*)-sabinene hydrate chemotype (U-type) was determined by enantioselective separation and identification by chiral-phase GC–MS. The numbers given are: 1a: (1*S*,2*S*,4*R*) (*E*)-sabinene hydrate, 1b: (1*R*,2*R*,4*S*) (*E*)-sabinene hydrate, 2a: (1*R*,2*S*,4*R*) (*Z*)-sabinene hydrate, 2b: (1*S*,2*R*,4*S*) (*Z*)-sabinene hydrate, 3a: (−)-(*S*)-α-pinene, 3b: (+)-(*R*)-α-pinene, 4a: (+)-(*R*)-β-pinene, 4b: (−)-(*S*)-β-pinene, 5a: (*S*)-α-terpineol and 5b: (*R*)-α-terpineol.

tected in the product profile of both enzymes. The opposite stereochemistry of TPS6 and TPS7 was also observed among all their minor chiral monoterpene products. For example, while TPS6 produced (−)-(*S*)-α-pinene, (−)-(*S*)-β-pinene and (*S*)-α-terpineol, TPS7 formed (+)-(*R*)-α-pinene, (+)-(*R*)-β-pinene and (*R*)-α-terpineol (Fig. 5B,C,D). In summary, the products of TPS6 and TPS7 displayed the opposite stereospecificity at C-4 (Fig. 6). The essential oil of the sabinene hydrate chemotype contained the stereoisomers of both enzymes, indicating that both terpene synthases contribute to the blend.

The stereochemistry of the terpene products is determined by the conformation of the LPP intermediate in the TPS6 and TPS7 reaction centers

In order to understand how the opposite stereoselectivity of TPS6 and TPS7 is determined, we first wanted to find out which step in the reaction is responsible for the crucial difference between both enzymes. Linalyl diphosphate is the earliest chiral reaction intermediate and has previously been utlilized to study the reaction mechanism of monoterpene synthases [9]. To test the stereospecific preference of TPS6 and TPS7 at this step of the reaction, we synthesized enantiopure (3*R*)-LPP and (3*S*)-LPP that we used as substrates. TPS6 and TPS7 accepted both enantiomers of LPP and converted them into the respective enantiomers of the monoterpenes (Fig. 7). When (3*R*)-LPP was offered, both enzymes converted it exclusively into (1*S*,2*S*,4*R*)-(*E*)-sabinene hydrate. Conversely, incubation with (3*S*)-LPP substrate resulted in (1*R*,2*R*,4*S*)-(*E*) and (1*S*,2*R*,4*S*)-(*Z*)-sabinene hydrate. The relatively high abundance of (1*S*,2*S*,4*R*)-(*E*)-sabinene hydrate after incubation with (3*S*)-LPP was most likely due to the fact that (3*S*)-LPP was not completely enantiopure, and contained approximately 10% (3*R*)-LPP (see 'Materials and Methods' section). As with the GPP substrate, the stereoisomer (1*R*,2*S*,4*R*)-(*Z*)-sabinene hydrate was not formed by the enzymes. The conformation of the minor monoterpene products also followed the chirality of the respective LPP substrate (Fig. S2).

To investigate the kinetic preferences for the reaction intermediate LPP, we performed enzyme assays with the (3*R*)-LPP substrate and determined the resulting product concentrations. TPS7 produced twice the concentration of the most abundant monoterpenes *trans*-sabinene hydrate, α-terpineol and limonene than TPS6, indicating a higher turnover of (3*R*)-LPP by TPS7.

Mutagenesis studies revealed an amino acid responsible for the different stereoselectivity of TPS6 and TPS7

The 85% amino acid identity between TPS6 and TPS7 provided an opportunity to identify the residue(s) responsible for the opposite stereoselectivity by sequence comparison and site-directed mutagenesis. The amino acid Asn-350 in TPS6 corresponds to Ile-346 in TPS7 (Fig. S3). Both residues were located seven amino acids upstream of the DDxxD motif. In a closely related 1,8-cineole synthase of the Lamiaceae *Salvia fruticosa*, the corresponding Asn-338 residue was demonstrated to be important for product specificity of the enzyme [18].

To test whether this residue can determine the stereoselectivity of TPS6 and TPS7, we altered Asn-350 of TPS6 to Ile, the corre-

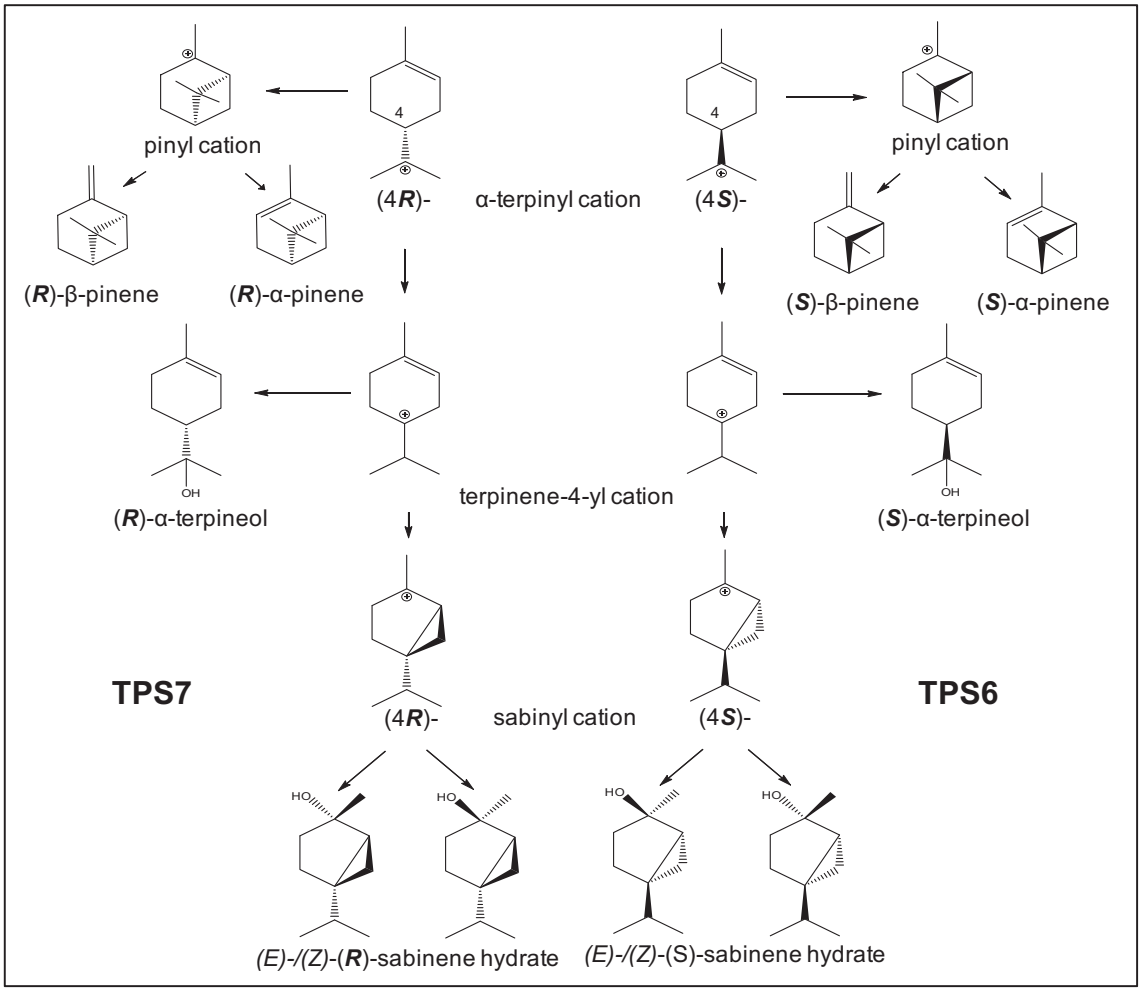

Fig. 6. Putative reaction mechanism of TPS6 and TPS7. The monoterpene products of TPS6 and TPS7 are derived from the α-terpinyl cation intermediates by cyclizations, hydride shifts, and termination by proton loss or quenching with water. TPS6 forms primarily monoterpenes of the *S*-configuration-series, whilst TPS7 forms monoterpenes of the *R*-configuration-series.

sponding amino acid in TPS7, by *in vitro* mutagenesis. After overexpression and incubation with GPP substrate, the N350I mutant of TPS6 altered its stereospecificity to that of TPS7 and produced only the (1*S*,2*S*,4*R*)-enantiomer of (*E*)-sabinene hydrate (Fig. 8). Conversely, the I346N mutant of TPS7 displayed a stereospecificity similar to that of TPS6. Although (1*S*,2*S*,4*R*)-(*E*)-sabinene hydrate was still the main product of this mutant, TPS7 I346N also produced the (4*S*)-enantiomers of (*E*)-sabinene hydrate and (*Z*)-sabinene hydrate.

Modeling of the TPS6/TPS7 active site

To illustrate the mechanism by which one amino acid, Asn-350 in TPS6 or Ile-346 in TPS7, can affect the stereospecificity of the reaction mechanism of the enymes, we created a model of the TPS6 and TPS7 active sites by threading of the sequences onto the structure of bornyl diphosphate synthase from *Salvia officinalis* [27]. The surface of the active site is formed by 31 amino acid residues, of which five residues differ between the enzymes (Fig. S3).

The GPP substrate was docked into the active-site pocket (Fig. 9). The model suggested that Asn-350 in TPS6 and Ile-346 in TPS7 were located at the bottom of the active site-cavity, in the middle of an α-helix that was designated as helix D in bornyl diphosphate synthase. The same helix accommodates also the magnesium-binding DDxxD-motif at the C-terminal end. The Asn-350 residue (TPS6) reached further into the active cavity than the Ile-346 residue (TPS7) and might favor the right-handed folding of the GPP substrate. The position of the GPP molecule would then result in the formation of the (3*S*)-LPP intermediate and determine the stereospecificity of the reaction products of TPS6. With an Ile residue in this position, the cavity might be bigger and the substrate could be more flexible. The left-handed conformation of the GPP might be energetically favored in the larger cavity and thereby preferred in TPS7. Also, the right-handed conformation of the substrate might be destabilized by specifc amino acid residues that change the steric or charge interactions in the active-site of TPS7.

Discussion

TPS6 and TPS7 may be responsible for the characteristic monoterpene composition of the sabinene hydrate chemotype of T. vulgaris

The essential oil of the sabinene hydrate chemotype of *T. vulgaris* is dominated by high concentrations of both (*E*)- and (*Z*)-sabinene hydrate. The two *T. vulgaris* terpene synthases, TPS6 and TPS7, produce not only sabinene hydrate but minor concentrations of 16 additional monoterpenes. Since TPS7 is expected to be more active than TPS6 due to its lower K_m value (K_m 6.1 μM and K_m 33.5 μM for GPP, respectively), the dominance of (1*S*,2*S*,4*R*)-*(E)*-sabinene

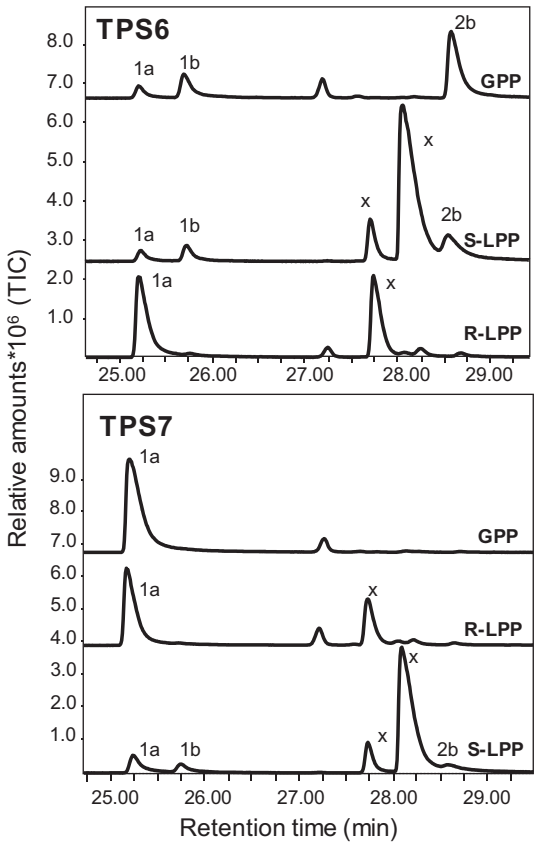

Fig. 7. The configuration of the monoterpene products is determined by the configuration of the LPP intermediate. The enantiomeric composition of TPS6 and TPS7 products after incubation with GPP, (3*R*)-LPP and (3S)-LPP was determined by GC–MS analysis on a chiral-phase column. The numbers given to the compounds refer to those of Fig. 5. The linalool detected in these traces is a substrate artifact (x).

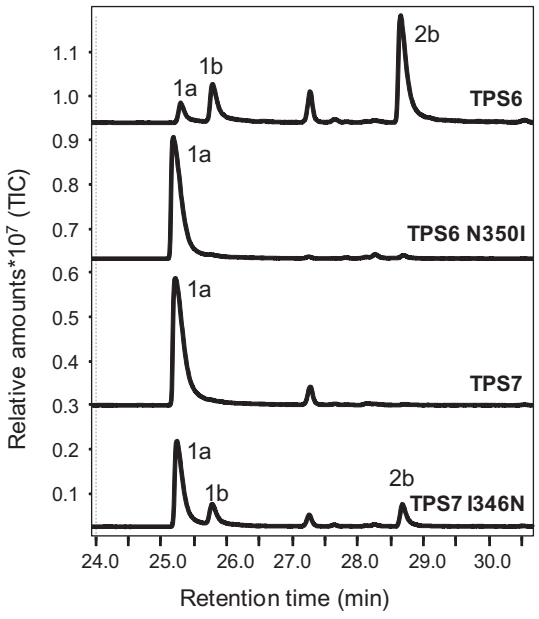

Fig. 8. Site-directed mutagenesis of a critical amino acid residue of TPS6 and TPS7 inverts the stereochemistry of the sabinene hydrate products. GC-traces show the enantiomeric composition of the products of both enzymes and their respective site-directed mutations. The numbers given refer to the compounds identified in Fig. 5.

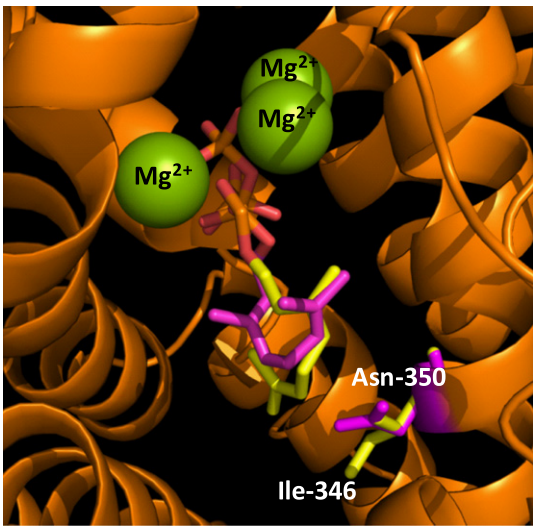

Fig. 9. Model of the TPS6 and TPS7 active sites. Both Asn-350 of TPS6 (shown in purple) and Ile-346 of TPS7 (shown in yellow) affect the conformation of the GPP substrate that is shown in the corresponding color. The trinuclear magnesium cluster is shown in green. (For interpretation of the references to color in this figure legend, the reader is referred to the web version of this article.)

hydrate in the essential oil seems reasonable. A quantitative model adjusting the product concentrations of both terpene synthases to fit the ratio of *(E)*- to *(Z)*-sabinene hydrate found in the essential oil demonstrates that the two enzymes are sufficient to produce nearly the complete monoterpene blend of the chemotype (Fig. 10). Only one monoterpene compound, *p*-cymene, appears to be an additional constituent of the oil. Most likely, *p*-cymene is derived from γ-terpinene, either by spontaneous conversion or through the action of a cytochrome P450 monooxygenase [33]. The concentration of terpinene-4-ol is higher in the essential oil than in the product spectra of TPS6 and TPS7. Most likely, terpinene-4-ol is formed non-enzymatically by rearrangement of sabinene hydrate which is produced in large amounts by both TPS6 and TPS7 [34]. The Neighbor-Joining dendrogram (Fig. 2) clusters TPS6 and TPS7 in the clade of monoterpene synthases of Lamiaceae, displaying the close relationship to terpene synthases from *Origanum vulgare*. This analysis confirms that sequence identity between terpene synthases from Lamiaceae is relatively high and not necessarily linked to catalytic function.

In addition to the monoterpenes, low concentrations of sesquiterpenes including (*E*)-β-caryophyllene, germacrene D and nerolidol were identified in *Thymus* species. These sesquiterpenes were found in most chemotypes of thyme and are most likely not affected by the mechanism of chemotype formation [35]. The characterization of sesquiterpene synthases in the closely related Lamiaceae *O. vulgare* suggests that two or three sesquiterpene synthases are sufficient to produce the complete sesquiterpene blend of the sabinene hydrate chemotype in thyme [36].

The initial conformation of GPP determines the opposite stereochemistry of TPS6 and TPS7

In terpene synthases, the succession of unstable carbon cation intermediates is responsible for the formation of multiple products [3]. Previous biochemical studies on the sabinene hydrate synthase activities in sweet majoram (*Majorana hortensis*) suggested that (*E*)- and (*Z*)-sabinene hydrate are not formed via sabinene or α-thujene intermediates [37]. Our characterization of TPS6 and TPS7 from thyme suggests that the reaction proceeds over the α-terpinyl cation, the terpinene-4-yl cation, and the sabinyl cation

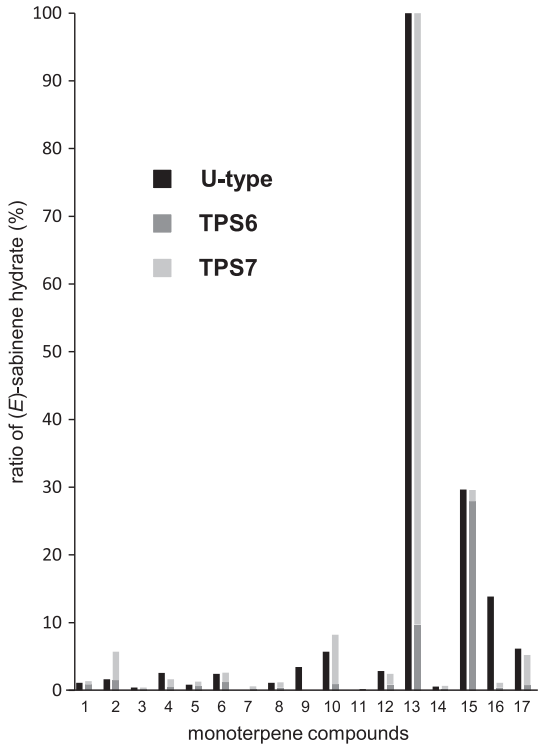

Fig. 10. The products of TPS6 and TPS7 are responsible for the monoterpene spectrum of the (*E*)-sabinene hydrate chemotype of *T. vulgaris*. The numbers given refer to the numbers in Table 1. The amount of *(E)*-sabinene hydrate was set as 100% in both the chemotype and the blend produced by TPS6 and TPS7. The ratio between *(E)*- and *(Z)*-sabinene hydrate in the chemotype was set as the same in the sum of TPS6 and TPS7. Therefore the amounts produced by TPS7 were multiplied with the factor 2,4. The relative amounts of the monoterpenes were calculated as a percentage of *(E)*-sabinene hydrate.

(Fig. 6). A striking feature of TPS6 and TPS7 is the opposite stereospecificity of their products. The presence of two terpene synthases with opposing stereospecificity has been observed in several other plants including the (−)-α-pinene synthase and (+)-α-pinene-synthase of loblolly pine [6] or the (+)germacrene D synthase and the (−)germacrene D synthase from goldenrod [38], and sesquiterpene synthases TPS4 and TPS5 from maize [39].

To identify the step of the reaction mechanism that introduces the stereoselectivity, we utilized (3*R*)- and (3*S*)-LPP as substrates. These likely pathway intermediates contain a stereocenter at C-3 which determines the configuration of all chiral monoterpene products. The ability of monoterpene synthases to control the stereochemistry indicates that the conversion of GPP to LPP is stereospecific and most likely influenced by the initial helical fold of the native substrate. According to this theory, the right-handed folding facilitates the formation of (3*S*)-LPP and the left-handed folding yields (3*R*)-LPP [9]. However, the enzymes are not capable of excluding the unfavored LPP enantiomers. This may be due to the fact that both configurations of the tertiary intermediate show similar hydrophobic properties, especially in the *anti-endo* conformation [8]. For the (−) bornyl diphosphate cyclase from tansy, a loss of function was reported when feeding with the unnatural LPP enantiomer [9].

One amino acid in the active site controls most of the stereospecificity of TPS6 and TPS7

The 85% sequence similarity between TPS6 and TPS7 enabled us to identify the structures in the active site that determine the stereospecificity of the reaction mechanism. A similar approach was successful with two terpene synthases in maize [39], while other pairs of stereoselective terpene synthases including (−)-α-pinene synthase and (+)-α-pinene-synthase of loblolly pine share a sequence identity of only 66% and are therefore not suitable for structure–function analyses [6].

In TPS6 and TPS7, a single amino acid located seven positions upstream the magnesium-binding DDxxD-sequence motif, Asn-350 in TPS6 and Ile-346 in TPS7, determined the stereospecificity of the enzymes and thus the binding conformation of GPP. The corresponding Asn-338 residue in a 1,8-cineole synthase of *S. fruticosa* was demonstrated to bind water that is used for product hydroxylation [18]. However, the formation of hydroxylated terpenes is not abolished by an isoleucine at the respective position in TPS7. To identify the amino acid residue(s) responsible for the binding of water in TPS6 and TPS7, we conducted a site-directed mutagenesis on six amino acid residues with polar or hydrophilic properties that were changed to nonpolar residues. Mutation of Y-432, E-435, S-457, R-498, D-501 and E-509 (numbers refer to TPS6) resulted in inactive enzymes, suggesting that these residues are important for protein stability or correct folding of the active-site. Due to the loss of overall activity, we could not determine whether these amino acid residues also participate in water quenching.

The model of the TPS6 and TPS7 reaction centers (Fig. 9) illustrates the likely binding conformations of the GPP substrate. According to this model, the steric interaction between the amino acid residue and the carbon moiety of the GPP appears to be crucial. In TPS6, the side chain of Asn-350 may force the GPP-molecule to form an upward kink while Ile-346 in TPS7 provides more space.

Thus, the two conformations illustrated in Fig. 9 could represent the right- and left-handed helical fold of GPP that determines the stereoselective reaction.

The mutation studies showed a complete reversal of stereospecificity when Ile was substituted by Asn-350 in TPS6. This might be explained by an increased space in the active center that allows for an energetically favored conformation of GPP or a steric clash of Ile with GPP in TPS6. In TPS7, the opposite substitution (Ile-346 to Asn) did not completely invert the product spectrum (Fig. 8). This indicates that Asn at this position in TPS7 causes the formation of equal amounts of both enantiomers of LPP. There are no obvious amino acid differences nearby to explain these relative effects since they are similar in size and chemical properties. Most likely, this effect is due to conformation changes of enzyme structure that are caused by distant amino acid residues.

The position of Asn-350 (TPS6) and Ile-346 (TPS7) supports the observation in a study of Köllner et al. [39], who located the crucial amino acids for stereospecificity in the terpene synthases TPS4 and TPS5 of maize also at the bottom of the active site. Also, Schwab et al. [40] compared the active-site openings of terpene synthases which generate antipodal configurations of LPP and recognized no significant differences. Thus, the mechanistic differences were assumed to reflect in structural differences deeper in the active-site pocket.

Interestingly, two stereoselective (*R*)-limonene synthases from *Schizonepeta tenuifolia* and *Agastache rugosa* contain an isoleucin residue seven amino acids upstream the DDxxD-motif while several (*S*)-limonene synthases of *Mentha longifolia*, *Mentha spicata*, *Perilla frutescens* and *Perilla citriodora* contain an asparagine residue at this position [41,42]. This indicates a general function of this amino acid position in the stereocontrol of terpene synthases.

Acknowledgment

We thank John Thompson for providing the *Thymus vulgaris* chemotypes.

Appendix A. Supplementary data

Supplementary data associated with this article can be found, in the online version, at http://dx.doi.org/10.1016/j.abb.2012.12.003.

References

[1] A. Zarzuelo, E. Crespo, The medicinal and non-medicinal uses of thyme, in: E. Stahl-Biskup, F. Sáez (Eds.), Thyme, The genus Thymus, Medicinal and Aromatic Plants – Industrial Profiles, Taylor & Francis, New York, 2002, pp. 263–292.
[2] P. Vernet, P.H. Gouyon, G. Valdeyron, Genetica 69 (1986) 227–231.
[3] E.M. Davis, R. Croteau, Top. Curr. Chem. 209 (2000) 53–94.
[4] J. Degenhardt, T.G. Köllner, J. Gershenzon, Phytochemistry 70 (2009) 1621–1637.
[5] C.L. Steele, J. Crock, J. Bohlmann, R. Croteau, J. Biol. Chem. 273 (1998) 2078–2089.
[6] A.P. Phillips, M.R. Wildung, D.C. Williams, D.C. Hyatt, R. Croteau, Arch. Biochem. Biophys. 411 (2003) 267–276.
[7] W.A. König, C. Fricke, Y. Saritas, B. Momeni, G. Hohenfeld, J. High Resolut. Chromatogr. 20 (1997) 55–61.
[8] D.M. Satterwhite, C.J. Wheeler, R. Croteau, J. Biol. Chem. 260 (1985) 13901–13908.
[9] R. Croteau, D.M. Satterwhite, D.E. Cane, C.C. Chang, J. Biol. Chem. 261 (1986) 13438–13445.
[10] C.M. Starks, K. Back, J. Chappell, J.P. Noel, Science 277 (1997) 1815–1819.
[11] D.W. Christianson, Chem. Rev. 106 (2006) 3412–3442.
[12] J. Bohlmann, G. Meyer-Gauen, R. Croteau, PNAS 95 (1998) 4126–4133.
[13] D.C. Williams, D.J. McGarvey, E.J. Katahira, R. Croteau, Biochemistry 37 (1998) 12213–12220.
[14] D.C. Hyatt, R. Croteau, Arch. Biochem. Biophys. 439 (2005) 222–233.
[15] R.J. Peters, R.B. Croteau, Arch. Biochem. Biophys. 417 (2003) 203–211.
[16] S. Katoh, D. Hyatt, R. Croteau, Arch. Biochem. Biophys. 425 (2004) 65–76.
[17] M.K. El Tamer, J. Lücker, D. Bosch, H.A. Verhoeven, F.W.A. Verstappen, W. Schwab, A.J. van Tunen, A.G.J. Vorhagen, R.A. de Maagd, H.J. Bouwmeester, Arch. Biochem. Biophys. 411 (2003) 196–203.
[18] S.C. Kampranis, D. Ioannidis, A. Purvis, W. Mahrez, E. Ninga, N.A. Katerelos, S. Anssour, J.M. Dunwell, J. Degenhardt, A.M. Makris, P.W. Goodenough, C.B. Johnson, Plant Cell 19 (2007) 1994–2005.
[19] J.D. Thompson, J.-C. Chalchat, A. Michet, Y.B. Linhart, B. Ehlers, J. Chem. Ecol. 29 (2003) 859–880.
[20] <http://www.ncbi.nlm.nih.gov/BLAST/> (accessed 09.01.12).
[21] S.C. Gill, P.H. von Hippel, Anal. Chem. 182 (1989) 319–326.
[22] R.P. Adams, Identification of Essential Oil Components by Gas Chromatography/Mass Spectrometry, fourth ed., Allured Publishing Corporation, Illinois, 2007.
[23] R.K. Keller, R. Thompson, J. Chromatogr. 645 (1993) 161–167.
[24] <http://www.expasy.org> (accessed 09.01.12).
[25] K. Arnold, L. Bordoli, J. Kopp, T. Schwede, Bioinformatics 22 (2006) 195–201.
[26] T. Schwede, J. Kopp, N. Guex, M.C. Peitsch, Nucleic Acids Res. 31 (2003) 3381–3385.
[27] D.A. Whittington, M.L. Wise, M. Urbansky, R.M. Coates, R. Croteau, D.W. Christianson, PNAS 99 (2002) 15375–15380.
[28] M.F. Sanner, J. Mol. Graphics Modell. 17 (1999) 57–61.
[29] O. Trott, A.J. Olson, J. Comput. Chem. 31 (2010) 455–461.
[30] The PyMOL Molecular Graphics System, Version 1.3, Schrödinger, LLC.
[31] <http://www.cbs.dtu.dk/services/> (accessed 09.01.12).
[32] M.L. Wise, R. Croteau, Monoterpene biosynthesis, in: D.E. Cane (Ed.), Comprehensive Natural Products Chemistry, Elsevier, Amsterdam, 1999, pp. 97–153.
[33] A. Keszei, C.L. Brubaker, W.J. Foley, Aust. J. Biol. 56 (2008) 197–213.
[34] C.P. Cornwell, D.N. Leach, S.G. Wyllie, J. Essent. Oil Res. 11 (1999) 49–53.
[35] E. Stahl-Biskup, Essential oil chemistry of the genus Thymus – a global view, in: E. Stahl-Biskup, F. Sáez (Eds.), Thyme, The genus Thymus, Medicinal and Aromatic Plants – Industrial Profiles, Taylor & Francis, New York, 2002, pp. 75–124.
[36] C. Crocoll, J. Asbach, J. Novak, J. Gershenzon, J. Degenhardt, Plant Mol. Biol. 73 (2010) 587–603.
[37] T.W. Hallahan, R. Croteau, Arch. Biochem. Biophys. 264 (1988) 618–631.
[38] C.O. Schmidt, H.J. Bouwmeester, S. Franke, W.A. König, Chirality 11 (1999) 353–362.
[39] T.G. Köllner, C. Schnee, J. Gershenzon, J. Degenhardt, Plant Cell 16 (2004) 1115–1131.
[40] W. Schwab, D.C. Williams, E.M. Davis, R. Croteau, Arch. Biochem. Biophys. 392 (2001) 123–136.
[41] T. Maruyama, M. Ito, F. Kiuchi, G. Honda, Biol. Pharm. Bull. 24 (2001) 373–377.
[42] T. Maruyama, D. Saeki, M. Ito, G. Honda, Biol. Pharm. Bull. 25 (2002) 661–665.